

# Increased endothelial and vascular smooth muscle cell adhesion on nanostructured titanium and CoCrMo

Saba Choudhary<sup>1</sup>  
Mikal Berhe<sup>1</sup>  
Karen M Haberstroh<sup>1</sup>  
Thomas J Webster<sup>1,2</sup>

<sup>1</sup>Weldon School of Biomedical Engineering and <sup>2</sup>School of Materials Engineering, Purdue University, West Lafayette, IN, USA

**Abstract:** In the body, vascular cells continuously interact with tissues that possess nanostructured surface features due to the presence of proteins (such as collagen and elastin) embedded in the vascular wall. Despite this fact, vascular stents intended to restore blood flow do not have nanoscale surface features but rather are smooth at the nanoscale. As the first step towards creating the next generation of vascular stent materials, the objective of this in vitro study was to investigate vascular cell (specifically, endothelial, and vascular smooth muscle cell) adhesion on nanostructured compared with conventional commercially pure (cp) Ti and CoCrMo. Nanostructured cp Ti and CoCrMo compacts were created by separately utilizing either constituent cp Ti or CoCrMo nanoparticles as opposed to conventional micron-sized particles. Results of this study showed for the first time increased endothelial and vascular smooth muscle cell adhesion on nanostructured compared with conventional cp Ti and CoCrMo after 4 hours' adhesion. Moreover, compared with their respective conventional counterparts, the ratio of endothelial to vascular smooth muscle cells increased on nanostructured cp Ti and CoCrMo. In addition, endothelial and vascular smooth muscle cells had a better spread morphology on the nanostructured metals compared with conventional metals. Overall, vascular cell adhesion was better on CoCrMo than on cp Ti. Results of surface characterization studies demonstrated similar chemistry but significantly greater root-mean-square (rms) surface roughness as measured by atomic force microscopy (AFM) for nanostructured compared with respective conventional metals. For these reasons, results from the present in vitro study provided evidence that vascular stents composed of nanometer compared with micron-sized metal particles (specifically, either cp Ti or CoCrMo) may invoke cellular responses promising for improved vascular stent applications.

**Keywords:** nanotechnology, metals, Ti, CoCrMo, vascular stents, endothelial cells, vascular smooth muscle cells

## Introduction

Vascular disease (including atherosclerosis or hardening of the arteries) is one of the leading causes of death in the world, affecting approximately 58 million people (National Institutes of Health 2005). Many treatment options are available for fighting atherosclerosis (including angioplasty, orally prescribed pharmaceutical agents, etc), but when plaque build-up becomes severe, implantation of vascular stents into stenosed arteries is a necessary treatment to help restore normal blood flow to ischemic organs (Hallisey et al 1992). Because they can prop open occluded arteries mechanically, metals (including Ti, stainless steel, Nitinol, and CoCr alloys) have been widely used as vascular stents (Robertson et al 2005). However, such conventional metals are generally not compatible with tissues, and the use of such metals as vascular stents can cause acute thrombosis and long-term restenosis

Correspondence: Thomas J Webster  
Division of Engineering, Brown  
University, 182 Hope Street, Providence,  
RI 02912, USA  
Tel +1 401 863 2677  
Fax +1 401 863 2676  
Email thomas\_webster@brown.edu

(Robertson et al 2005). It is for these reasons that numerous investigators are modifying traditional metals used as vascular stents by creating coatings composed of silicon carbide (Schuler et al 2003), expanded-polytetrafluoroethylene (Cejna et al 2002), tantalum (Chen et al 2002), and hyaluronan (Pitt et al 2004). All these coatings are showing promise towards improving interactions with cells necessary for the next generation of more successful vascular stents. Specifically, functions of vascular smooth muscle and endothelial cells that integrate the stent into juxtaposed vascular tissue should be supported while interactions with platelets (which can cause the formation of a platelet-plug that limits blood flow) should be inhibited on a successful vascular stent.

However, due to blood flow, coatings may delaminate under normal shear stresses imposed on a vascular stent which would cause complications downstream. Considering this, few attempts have been made to alter the original surface of metallic vascular stents to optimally interact with cells. A recent approach that has centered on modifying a vascular stent surface creates a unique nanometer topography that mimics that of the natural vascular tissue. To demonstrate the unique nanostructured features present in vascular tissue, Fleming et al (1996) created a polymethylmethacrylate (PMMA) mold of a denuded canine artery (Figure 1). As was demonstrated, endothelial and vascular smooth muscle cells residing in vascular tissue are clearly accustomed to interacting with surfaces with a high degree of nanometer features (Fleming et al 1996). Despite this fact, most vascular stents currently being used and

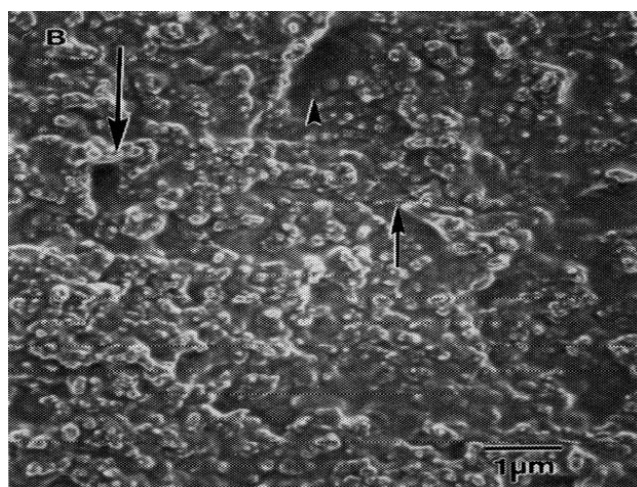


**Figure 1** Nanometer roughness of vascular tissue. Previous studies have demonstrated highly irregular nanostructured surface features yet to be duplicated in metals used as vascular stents. Scale bar = 1  $\mu\text{m}$ . Source: Fleming RG, Murphy CJ, Abrams GA, et al. 1996. Effects of synthetic micro- and nanostructured surfaces on cell behavior. *Biomaterials*, 17:2087–95. Copyright © 1996. Obtained and reprinted with permission from Elsevier.

proposed do not have nanoscale surface features (such as protrusions, ridges, grooves). Such surfaces do not promote endothelial cell adhesion and, therefore, do not encourage the formation of an endothelial cell monolayer that would inhibit platelet attachment on vascular stent walls.

Although mimicking the nanostructured roughness of vascular tissue in metals has remained largely unattempted for stent applications, some investigators have witnessed improved vascular cell functions on polymers with biologically inspired nanostructured features (Miller et al 2004, 2005). For example, Miller et al (2004) measured increased endothelial and vascular smooth muscle cell functions on poly-lactic-co-glycolic acid (PLGA), poly-etherurethane (PU), and polycaprolactone (PCL) with nanostructured compared with conventional (or smooth at the nanoscale) surface features. To accomplish this, soluble PLGA, PU, and PCL were separately poured into silastic molds possessing numerous nanometer surface features; the polymers were then allowed to cure. Compared with respective polymers smooth at the nanoscale, in vitro results showed over 4, 3, and 2 times the number of endothelial cells adherent on nanostructured PLGA, PU, and PCL after just 4 hours (Miller et al 2004). Similar enhanced vascular cell functions have been measured on nanostructured polymers created by polymer demixing (Dalby et al 2002) and lithography (Iwanaga et al 2005).

Although numerous techniques exist to create nanometer surface features on polymers, relatively few exist for metals. It was for these reasons that the present study sought to determine techniques for creating nanostructured surface features on two commonly used vascular stent metals: commercially pure (or cp) Ti and CoCrMo. The present in vitro study also determined vascular cell (specifically, endothelial and vascular smooth muscle cell) adhesion on such nanostructured metal surfaces compared with conventionally used metals. In doing so, results of this study demonstrated for the first time greater endothelial and vascular smooth muscle cell adhesion on both cp Ti and CoCrMo possessing nanostructured compared with conventional surface features.

## Materials and methods

### Materials selection and synthesis of compacts

The objective of the material-synthesis phase was to generate nanostructured surface features on two metals that are currently used in vascular stent applications. Concerns of surface chemistry alterations – a possible effect of exposing

**Table 1** Metal particles<sup>a</sup>

Category	ASTM designation	Particle size	Particle shape
Nanostructured cp Ti	F-67; G2	250–750 nm	Spongy
Conventional cp Ti	F-67; G2	> 10.5 $\mu$ m	Spongy
Nanostructured CoCrMo	F-75; F-799	200–400 nm	Spherical and irregular mix
Conventional CoCrMo	F-75; F-799	14–16 $\mu$ m	Spherical and irregular mix

<sup>a</sup> Metal particles with dimensions less than and greater than 1  $\mu$ m were classified as nanostructured and conventional, respectively. Additionally, as determined by atomic force microscopy, metal nanoparticles provided for increased nanometer surface roughness.

fine particulates of reactive metals to unprotective, oxidizing, or contaminated atmospheres at elevated temperatures – were avoided by creating powder metallurgy compacts in the absence of heat. Specific interest was directed on those materials that are designed for processing via powder metallurgy techniques.

Two popular metals used in vascular stents are cp Ti and CoCrMo. cp Ti and CoCrMo metal particulates were purchased from Metal Alloy, Inc (Albany, NY, USA). Details of cp Ti and CoCrMo metal particulates used for creating nanostructured and conventional metal compacts are provided in Table 1. The metal particles were characterized by Metal Alloy, Inc.

Powders were loaded into a steel-tool die to obtain compacts for use in cell experiments according to standard techniques (Webster and Ejiófor 2004). Specifically, one pressure level (10 GPa over 5 minutes) was used to press the metal particles to green as-pressed densities 90%–95% of theoretical. All pressed green discs (diameter: 12 mm, thickness: 0.50–1.10 mm) were produced using a simple uniaxial, single-ended compacting hydraulic press (Carver Inc, Chicago, IL, USA). Particles were pressed in air at room temperature.

Rolled, heat-treated, and pickled cp Ti sheets (wrought Ti; Osteonics, Boston, MA, USA) were used as controls during the cell experiments. Lastly, tissue-culture polystyrene (Fisher, Chicago, IL, USA) was utilized as a reference substrate in the cell experiments. All substrates were sterilized by UV exposure for 1 hour on each side.

## Surface characterization

### Roughness

The surfaces of the metal compacts were characterized for roughness using scanning electron microscopy (SEM) and atomic force microscopy (AFM). For SEM, substrates were first sputter-coated with a thin layer of gold-palladium using

a Hummer I Sputter Coater (Technics, Chicago, IL, USA) in a 100 millitorr vacuum argon environment for a 3-minute period and at 10 mA of current. Images were taken using a JEOL JSM-840 Scanning Electron Microscope (JEOL, Chicago, IL, USA) at a 5 kV accelerating voltage. Digital images were recorded using Digital Scan Generator Plus (JEOL) software. For wrought Ti (reference), samples were also treated in an acidified (HF + HNO<sub>3</sub>) aqueous environment to reveal grain sizes; images of the wrought Ti control were obtained using both SEM and an optical microscope (Leica, Chicago, IL, USA).

For AFM, a NanoScope IIIa Atomic Force Microscope with NanoScope imaging software (Digital Instruments, Inc, Dallas, TX, USA) was used to quantify surface roughness and surface area. A scan rate of 2 Hz and 512 scanning points were used to obtain root-mean-square (rms) roughness values of 1 by 1  $\mu$ m AFM scans. All scans were performed in ambient air (at 15%–20% humidity). Experiments were completed in triplicate at three separate times.

### Chemistry

Electron spectroscopy for chemical analysis (ESCA) was performed on all substrates of interest to the present study using a Surface Science Instruments (SSI, Seattle, WA, USA) X-Probe. An aluminum K<sub>1,2 $\alpha$</sub>  monochromatized x-ray source was used to stimulate photoemission of the inner shell electrons of the sample. The energy of this electron was then recorded and analyzed for identification. Wide scans of the sample were used to generate low-resolution spectra that identified and quantified the percentages of different elements on the surface of the materials (approximately up to 100 Å deep) (Cooke et al 1996).

## Cell experiments

### Cells

Rat aortic endothelial cells were purchased from VEC Technologies (Greenbush, NY, USA), cultured in MCDB-131 Complete Medium (VEC Technologies) under standard cell culture conditions (ie, a 37°C, humidified, 5% CO<sub>2</sub>/95% air environment), and were used without further characterization in all experiments. Rat aortic smooth muscle cells were purchased from VEC Technologies, cultured in Dulbecco's Modified Eagle Medium (DMEM, Hyclone, Dallas, TX, USA) supplemented with 10% fetal bovine serum (FBS, Hyclone) and 1% penicillin/streptomycin (Hyclone) under standard culture conditions, and were used without further characterization in all experiments.

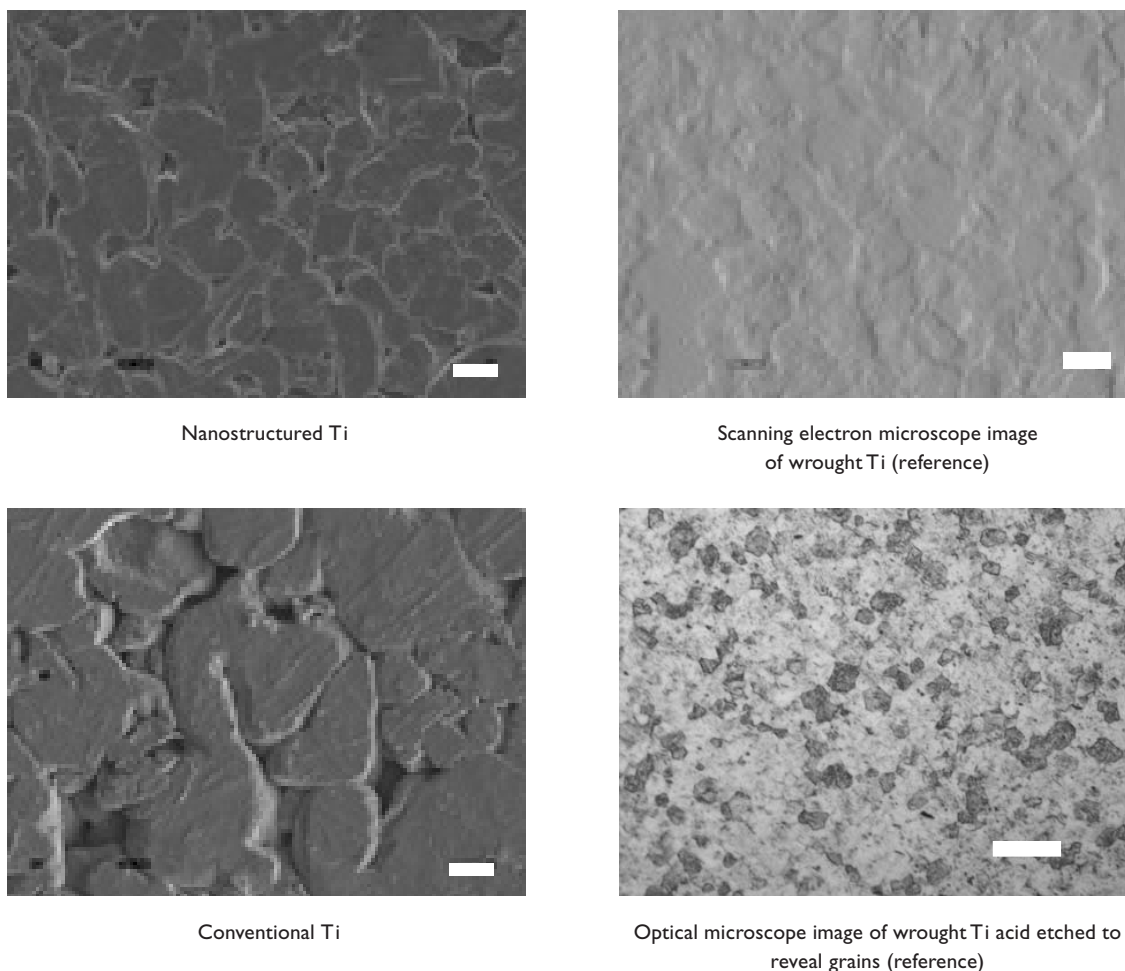


**Figure 2** Scanning electron microscopy images of cp Ti compacts. Increased nanostructured surface roughness was observed on nanostructured compared with conventional cp Ti. Bar = 1  $\mu\text{m}$  for nanostructured cp Ti and 10  $\mu\text{m}$  for conventional cp Ti. In contrast to nanostructured cp Ti, scanning electron microscopy images of wrought Ti indicated a large degree of microsurface roughness. Acidic etching of the wrought Ti samples revealed grain sizes 20–50  $\mu\text{m}$  (roughly equivalent to ASTM nr 7.5) under optical microscopy. Bar = 10  $\mu\text{m}$  for wrought Ti (reference), and 50  $\mu\text{m}$  for wrought Ti acid etched to reveal grain sizes.

### Cell adhesion and viability

Cell adhesion was determined because for anchorage-dependent cells, adhesion is imperative for subsequent cell functions like proliferation and synthesis of an extracellular matrix. Most importantly, endothelial cell adhesion is necessary to completely cover a metallic vascular stent and, therefore, protect it from detrimental blood cell (like platelet and leukocyte) interactions that could limit blood flow. To analyze this adhesion, endothelial and vascular smooth muscle cells were separately seeded (4500 cells/cm<sup>2</sup> substrate nominal surface area) in respective media and were allowed to adhere for 4 hours. At the end of the prescribed time period, non-adherent cells were removed by rinsing in phosphate buffered saline, and the viability of the adherent cells was determined using a live/dead assay according to manufacturer's instructions (Molecular Probes, Chicago, IL, USA). The numbers of live (stained fluorescent green) and dead (stained fluorescent red) cells were quantified and

reported as cells/cm<sup>2</sup>. Images were also obtained (using Image Pro, New York, NY, USA) to ascertain differences in cell spreading (specifically, length to width ratios and cell areas) on the substrates of interest. Experiments were completed in triplicate at three separate times.

### Statistics

Standard statistical tests (ANOVA followed by Duncan's Multiple Range Test) were performed to determine differences between means;  $p < 0.01$  was used.

## Results

### Surface characterization

Results provided evidence of increased nanometer surface roughness for nanostructured compared with conventional cp Ti (Figure 2) and CoCrMo (Figure 3). Please note the differences in the scale bars in these images to emphasize

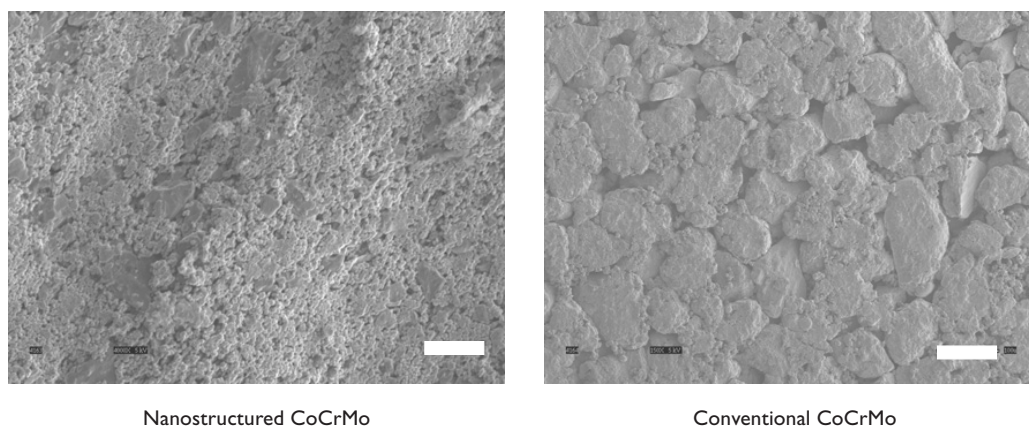


**Figure 3** Scanning electron microscopy images of CoCrMo compacts. Increased nanostructured surface roughness was observed on nanostructured compared with conventional CoCrMo. Bar = 1  $\mu\text{m}$  for nanostructured CoCrMo and 10  $\mu\text{m}$  for conventional CoCrMo.

the large differences in surface-feature magnitudes present on nanostructured compared with conventional metals. Unlike the corresponding conventional metal compacts, the dimensions of nanometer particles at the surface of nanostructured metals gave rise to larger amounts of interparticulate voids (with fairly homogeneous distributions). Conventional metals revealed smaller amounts of interparticulate voids with a non-homogeneous distribution.

The exposed topography of the wrought Ti sheet (reference substrate; Figure 2) showed surface features in the range of 20–60  $\mu\text{m}$ . Moreover, after etching in an acidic ( $\text{HF} + \text{HNO}_3$ ) aqueous solution, wrought Ti displayed grain sizes in the traditional range of 20–50  $\mu\text{m}$  (roughly equivalent to ASTM nr 7.5) under optical microscopy (Figure 2).

AFM data confirmed the increased nanometer surface roughness of the nanostructured compared with conventional metals (Table 2). Specifically, 2.4 and 4 times the amount of nanometer root-mean-square (rms) surface roughness was measured for nanostructured compared with conventional cp Ti and CoCrMo, respectively. Due to this increase in surface roughness, greater surface area (4.75 and 8 times) was also measured for the nanostructured compared with conventional cp Ti and CoCrMo, respectively. As

**Table 2** Surface properties of metal compacts

Category	Surface roughness (rms; nm)	Surface area (% increase compared with nominal surface area)
Nanostructured cp Ti	11.9 $\pm$ 2.2	19 $\pm$ 1.9
Conventional cp Ti	4.9 $\pm$ 1.4	4 $\pm$ 0.9
Nanostructured CoCrMo	14.1 $\pm$ 2.5	25 $\pm$ 3.1
Conventional CoCrMo	3.2 $\pm$ 0.2	3 $\pm$ 0.7
Wrought Ti	1.1 $\pm$ 0.1	1 $\pm$ 0.1

expected, the wrought Ti was extremely smooth at the nanometer level and had the lowest surface roughness (1.1 nm rms) of any of the metal substrates tested in this study.

Lastly, ESCA results provided evidence of similar elemental percentages of Ti and O on the surface of nanostructured compared with conventional cp Ti and wrought Ti (Table 3); specifically, as expected, each had the stoichiometric ratio of  $\text{TiO}_2$ . Similar chemistries were also measured between nanostructured and conventional CoCrMo (Table 4). This provided evidence of only altered surface roughness between all of the respective metal substrates tested in this study. Importantly, no impurities were found for any of the nanostructured or conventional metal compacts using ESCA.

## Cell experiments

Results of the present study provided the first evidence of increased endothelial cell adhesion on nanostructured compared with conventional cp Ti (Figure 4) and CoCrMo (Figure 6). Specifically, compared with conventional

**Table 3** Surface chemistry of cp Ti compacts

Category	Elemental composition (%)	
	Ti	O
Nanostructured cp Ti	31.7 $\pm$ 8.5	68.3 $\pm$ 3.8
Conventional cp Ti	32.4 $\pm$ 6.1	67.6 $\pm$ 5.9
Wrought Ti	33.5 $\pm$ 5.1	66.5 $\pm$ 6.2

**Table 4** Surface chemistry of CoCrMo compacts

Category	Elemental composition (%)		
	Co	Cr	Mo
Nanostructured CoCrMo	63.5 $\pm$ 9.2	25.1 $\pm$ 4.7	11.4 $\pm$ 3.0
Conventional CoCrMo	62.1 $\pm$ 8.8	24.9 $\pm$ 4.5	13.0 $\pm$ 2.2

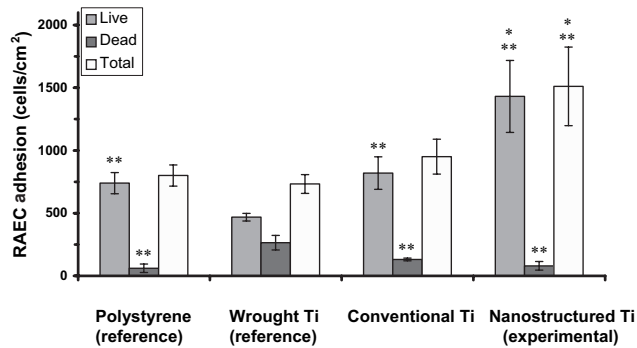


**Figure 4** Increased rat aortic endothelial cell (RAEC) adhesion on nanostructured cp Ti. Data = mean ± SEM; n = 3; \*p < 0.01 compared with respective conventional cp Ti and \*\*p < 0.01 compared with wrought Ti (reference).

formulations, the number of viable endothelial cells was almost 2 and 1.6 times greater on nanostructured cp Ti and CoCrMo, respectively. Compared with wrought Ti and tissue culture polystyrene, the number of viable endothelial cells was significantly (p < 0.01) greater on both nanostructured and conventional cp Ti as well as CoCrMo. Interestingly, the total number of endothelial cells was statistically similar between wrought Ti and conventional cp Ti, but significantly (p < 0.01) greater on conventional CoCrMo compared with wrought Ti. Importantly, compared with wrought Ti, the number of non-viable cells significantly (p < 0.01) decreased on both nanostructured and conventional cp Ti, but were significantly (p < 0.01) less only on nanostructured CoCrMo. Lastly, endothelial cell numbers were significantly (p < 0.01) higher on both types of CoCrMo (conventional and nanostructured) compared with respective cp Ti formulations.

Similar trends of increased (p < 0.01) numbers of vascular smooth muscle cells were observed on nanostructured compared with conventional cp Ti (Figure 5) and CoCrMo

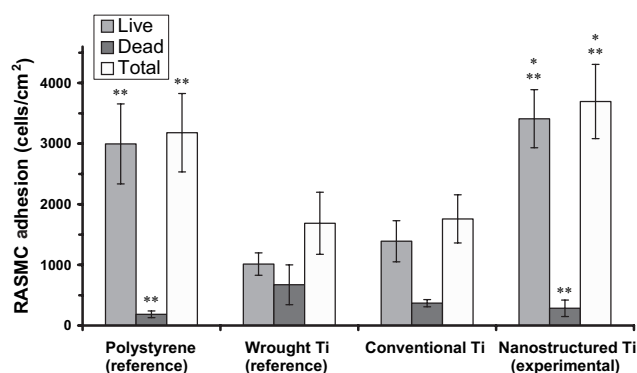


**Figure 5** Increased rat aortic smooth muscle cell (RASMC) adhesion on nanostructured cp Ti. Data = mean ± SEM; n = 3; \*p < 0.01 compared with respective conventional cp Ti and \*\*p < 0.01 compared with wrought Ti (reference).

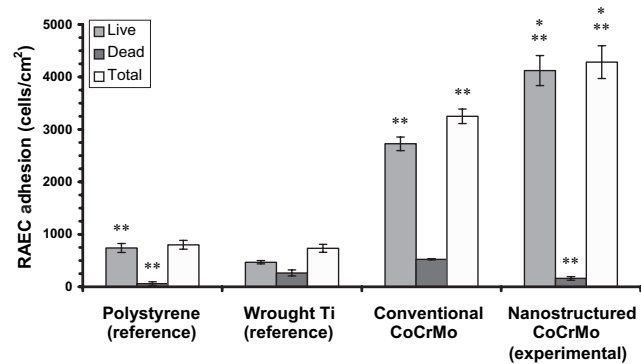


**Figure 6** Increased rat aortic endothelial cell (RAEC) adhesion on nanostructured CoCrMo. Data = mean ± SEM; n = 3; \*p < 0.01 compared with respective conventional CoCrMo and \*\*p < 0.01 compared with wrought Ti (reference).

(Figure 7). Specifically, compared with conventional formulations, the number of viable vascular smooth muscle cells increased almost 2.5 and 0.33 times on nanostructured cp Ti and CoCrMo, respectively. In contrast to trends observed with endothelial cells, compared with wrought Ti, the total number of vascular smooth muscle cells was significantly (p < 0.01) greater on both types of nanostructured metals but only on conventional CoCrMo; that is, vascular smooth muscle cell total numbers were similar between wrought Ti and conventional cp Ti. Viable endothelial numbers were significantly (p < 0.01) greater on both types of CoCrMo compared with wrought Ti. Lastly, similar to endothelial cells, more vascular smooth muscle cells adhered on both types of CoCrMo compared with respective cp Ti formulations.

When these results are considered in conjunction, the ratio of viable endothelial to vascular smooth muscle cells slightly increased (0.5 compared with 0.47) on nanostructured compared with conventional cp Ti; both were greater than on wrought Ti (0.44). More impressively, the

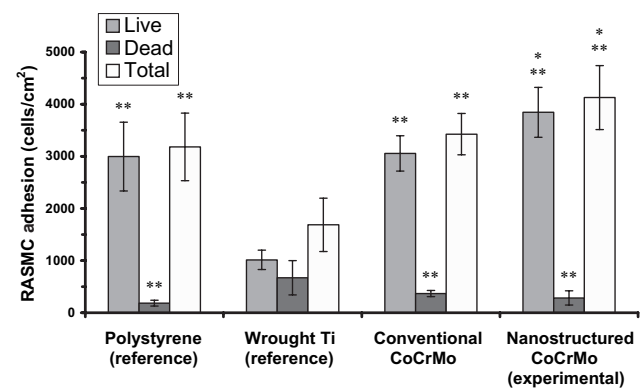


**Figure 7** Increased rat aortic smooth muscle cell (RASMC) adhesion on nanostructured CoCrMo. Data = mean ± SEM; n = 3; \*p < 0.01 compared with respective conventional CoCrMo and \*\*p < 0.01 compared with wrought Ti (reference).

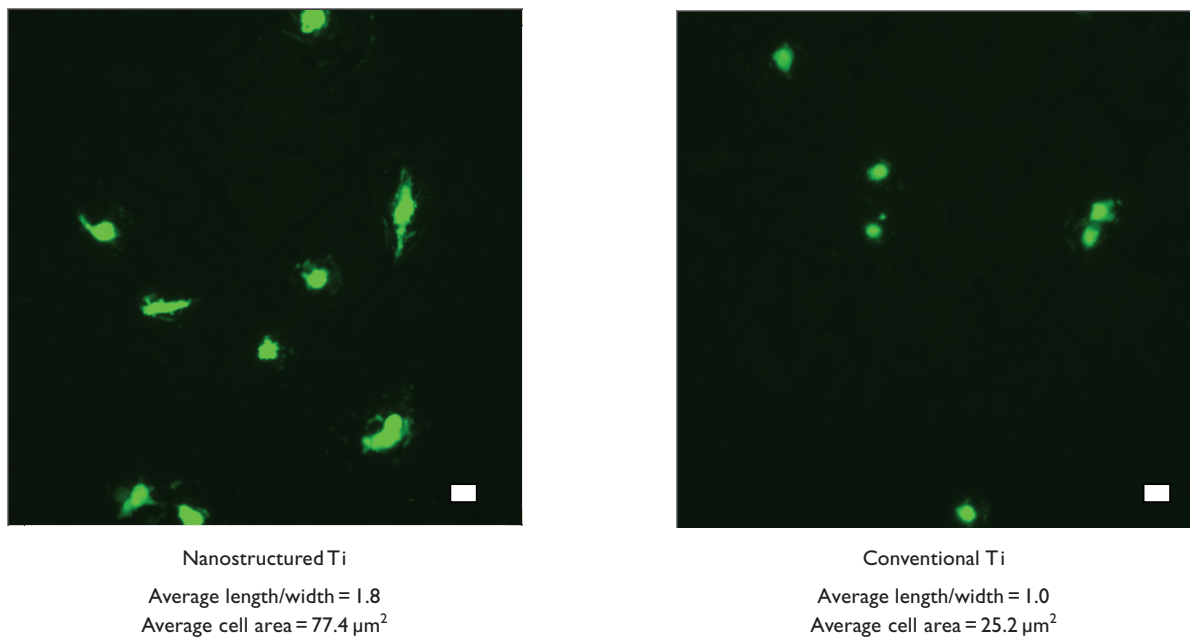


**Figure 8** Increased rat aortic endothelial cell (RAEC) spreading on nanostructured cp Ti. Scale bar = 10  $\mu\text{m}$ .

ratio of viable endothelial to vascular smooth muscle cells increased (1.08 compared with 0.86) on nanostructured compared with conventional CoCrMo. Also, the ratio of endothelial cells to vascular smooth muscle cells was much greater on both types of CoCrMo compared with respective cp Ti formulations. This result is important because previous studies have implied that greater numbers of vascular smooth muscle cells compared with endothelial cells in the vascular lumen leads to intimal hyperplasia (a major mode of stent failure; Messer et al 2005).

Lastly, images of endothelial and vascular smooth muscle cell morphology confirm quantitative studies (Figures 8 and 9 for endothelial and vascular smooth muscle cell morphology on cp Ti, respectively); similar results were observed on CoCrMo (data not shown). Specifically, both cell types were more well spread on the nanostructured compared with conventional metals. Since previous studies have correlated a better spread cell morphology with greater subsequent cell functions (such as proliferation and formation of an extracellular matrix) (Miller et al 2004,

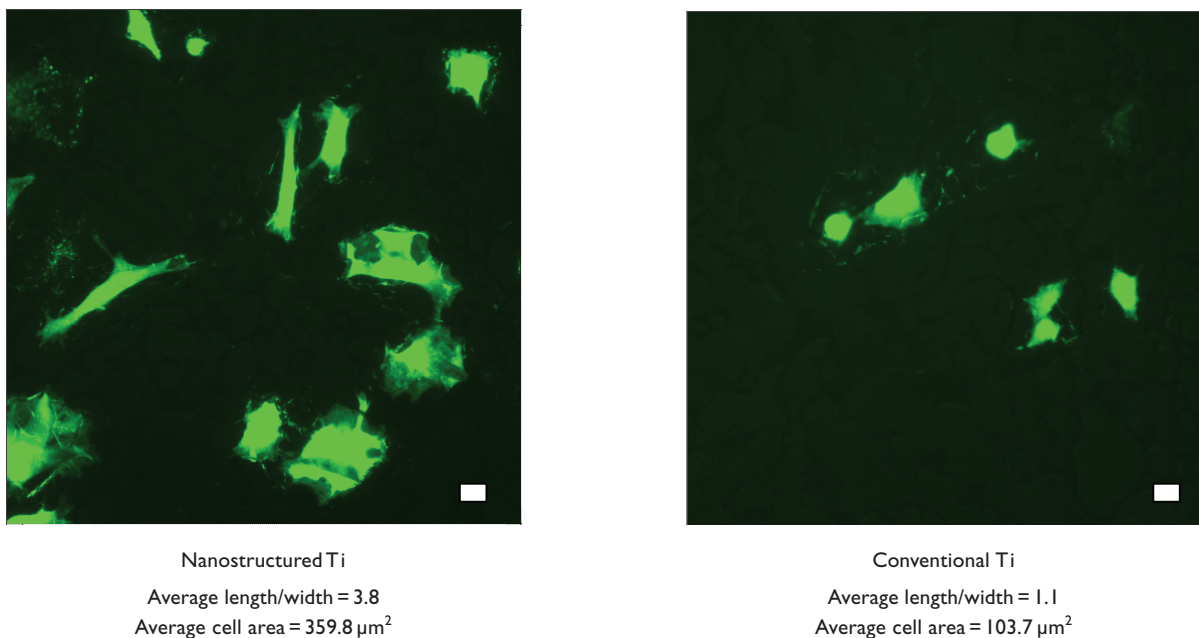


**Figure 9** Increased rat aortic smooth muscle cell (RASMC) spreading on nanostructured cp Ti. Scale bar = 10  $\mu\text{m}$ .

2005), such data imply greater subsequent vascular cell functions on nanostructured metals; however, more experiments are clearly needed to confirm this. Moreover, compared with conventional metals, results for greater endothelial cell spreading provided further evidence of a possible increased coverage of the luminal surface of a vascular stent composed of nanostructured metals. Greater coverage of the inside of a vascular stent by endothelial cells would protect the underlying metal surface from detrimental interactions with blood cells (such as leukocyte and platelet attachment) that could lead to blockage of blood flow.

## Discussion

For the first time, this study represents an attempt to advance design criteria for improving vascular cell function on polymers (Miller et al 2004, 2005; Dalby et al 2002; Iwanaga et al 2005) to metals. In doing so, the present study adds metals to the growing list of materials that, when created to possess nanometer surface features (through the use of constituent nanometer particulates), enhance endothelial and vascular smooth muscle cell adhesion. That is, compared with respective conventional counterparts, the presently studied cp Ti and CoCrMo as well as the previously studied polymers (specifically, PLGA, PU, and PCL; Miller et al 2004, 2005) all increased vascular cell responses when implementing nanostructured surface features. Thus, these results add to the argument that vascular cell attachment may be promoted regardless of material chemistry as long as a large degree of nanometer surface roughness is created. Since it is imperative to fully integrate a vascular stent with juxtaposed tissue to limit metal exposure to blood cells (like platelets) and avoid vessel occlusion, greater vascular cell attachment that may lead to such incorporation shows great promise towards improving the functions of metals as vascular stents.

The concept of creating stents with decreased surface feature dimensions (ie, into the nanometer regime) in order to mimic the roughness of vascular tissue has also been utilized by others (Gao et al 1998; Sung et al 2005). In such studies, the modified synthetic materials not only altered in their degree of nanometer surface roughness, but also in their chemistry, which may have also influenced vascular cell functions. For example, it has been reported that polyglycolic acid treated with NaOH to create smaller-dimensioned fibers promotes vascular smooth muscle cell functions (Gao et al 1998). Although this represents a novel

finding, due to chemistry changes that may have occurred during NaOH treatment (for example, ester bond breakage), it was not clear which property (chemistry or surface roughness) increased functions of vascular smooth muscle cells in that study.

This investigation was specifically designed to provide direct evidence of whether nanostructured cp Ti and CoCrMo influences vascular cell attachment solely due to nanometer surface roughness characteristics. Since metal particulates were chosen with similar respective chemistries and these particles were pressed without the use of heat, vascular cell adhesion was compared between metals of the same chemistry but vastly different degrees of nanometer surface roughness. Importantly, the type of nanometer surface features present in the metals investigated here can be changed by altering constituent particle shape and size; this should be the focus of future studies to optimize nanostructured surface features that enhance vascular cell adhesion.

It is intriguing to ponder why vascular cell adhesion increased on the metal surfaces with higher degrees of biologically inspired nanometer features. Since nanophase metals are composed of smaller particles of the same atoms compared with their conventional forms (which contain several billions of atoms and have particle sizes microns to millimeters in diameter), nanophase metals have unique surface properties (Siegel 1996). Specifically, nanophase metals have higher numbers of atoms at the surface compared with bulk, greater areas of surface defects (such as edge/corner sites and particle boundaries), and larger proportions of delocalized surface electrons (Klabunde et al 1996). Such altered surface properties will influence initial protein interactions that control subsequent cell adhesion.

In fact, investigations of the underlying mechanisms of increased vascular cell adhesion on nanostructured polymers revealed that the initial adsorbed concentration, conformation, and bioactivity of proteins contained in serum was responsible (Miller et al 2004, 2005). For example, by just decreasing polymer surface feature sizes to below 100 nm, select competitive fibronectin adsorption increased almost 10% on nanostructured PLGA formulations; this may in part have promoted vascular cell adhesion on nanostructured PLGA. In addition, greater unfolding of fibronectin was measured on nanostructured than on conventional PLGA by AFM. Increased unfolding of fibronectin may have promoted the availability of specific cell-adhesive epitopes (such as the amino acid sequence: Arg-Gly-Asp or RGD) to promote vascular cell adhesion.



Although experiments would be needed to verify this, the same events of optimal initial protein interactions for enhancing vascular cell adhesion may be happening on the presently studied nanostructured cp Ti and CoCrMo. Regardless of the mechanism, this study provides evidence that nanostructured cp Ti and CoCrMo should be further studied for improved vascular stent applications.

Lastly, it is important to mention that in the orthopedic community, studies have been also conducted on the same nanostructured cp Ti and CoCrMo investigated here. Specifically, increased osteoblast (bone-forming cell) functions have been measured on nanostructured compared with conventional cp Ti, Ti6Al4V, and CoCrMo (Webster and Ejiófor 2004). Compared with conventional metals, compacts composed of spherical nanometer particles of cp Ti, Ti6Al4V, and CoCrMo enhanced the adhesion of osteoblasts while at the same time decreased the adhesion of fibroblasts (cells that contribute to fibrous encapsulation and callus formation events that may lead to orthopedic implant loosening and failure). Increased functions of fibroblasts are also detrimental to vascular stents as they preclude the stent from integrating into juxtaposed vascular tissue. In addition, calcium deposition by osteoblasts was 3, 3, and 2 times greater when cultured on nanostructured compared with conventional cp Ti, Ti6Al4V, and CoCrMo after 28 days, respectively. Thus, this present study, considered in conjunction with these previous studies, suggests that nanostructured cp Ti and CoCrMo are able to improve the functions of numerous implantable devices.

## Conclusions

The present in vitro study provided the first evidence of greater endothelial and vascular smooth muscle cell adhesion on cp Ti and CoCrMo compacts with nanometer compared with conventionally sized particles; CoCrMo enhanced vascular cell adhesion more than cp Ti. Respective metal formulations had similar chemistry and altered only in degree of nanometer roughness. Both types of vascular cells were also shown to spread to a larger degree on nanostructured compared with conventional metals. Since nanostructured metals have higher percentages of particle boundaries at the surface, altered initial protein interactions may be responsible for the observed greater numbers of vascular cells on nanostructured compared with conventional metals. Since adhesion is a necessary prerequisite for subsequent functions of vascular cells (such as proliferation and the synthesis of an extracellular matrix),

these results suggest for the first time the promise nanostructured metals may have in vascular stent applications, although clearly this needs to be the focus of future studies.

## Acknowledgments

The authors would like to thank the National Science Foundation (#0304521) for funding.

## References

- Cejna M, Virmani R, Jones R, et al. 2002. Biocompatibility and performance of the Wallstent and the Wallgraft, Jostent, and Hemobahn stent-grafts in a sheep model. *J Vasc Interv Radiol*, 13:823–30.
- Chen JY, Leng YX, Tian XB, et al. 2002. Antithrombogenic investigation of surface energy and optical bandgap and hemocompatibility mechanism of Ti (Ta(+5)O<sub>2</sub>) thin films. *Biomaterials*, 23:2545–52.
- Cooke FW, Lemons JE, Ratner BD. 1996. In Ratner BD (ed). *Biomaterials science: an introduction to materials in medicine*. California: Academic Pr. p 11–35.
- Dalby MJ, Riehle MO, Johnstone H, et al. 2002. In vitro reaction of endothelial cells to polymer demixed nanotopography. *Biomaterials*, 23: 2945–54.
- Fleming RG, Murphy CJ, Abrams GA, et al. 1996. Effects of synthetic micro- and nanostructured surfaces on cell behavior. *Biomaterials*, 17:2087–95.
- Gao J, Nikalson L, Langer R. 1998. Increased vascular smooth muscle cells on NaOH treated PLGA. *J Biomed Mater Res*, 42:417–24.
- Hallisey MJ, Parker BC, van Breda A. 1992. Current status and extended applications of intravascular stents. *Curr Opin Radiol*, 4(4):7–12.
- Iwanaga S, Akiyama, Kikuchi A, et al. 2005. Fabrication of a cell array on ultrathin hydrophilic polymer gels utilizing electron beam irradiation and UV excimer laser ablation. *Biomaterials*, 26:5395–404.
- Klabunde KJ, Strak J, Koper O, et al. 1996. Nanocrystals as stoichiometric reagents with unique surface chemistry. *J Phys Chem*, 100:12141.
- Messer RL, Wataha JC, Lewis JB, et al. 2005. Effect of vascular stent alloys on expression of cellular adhesion molecules by endothelial cells. *J Long Term Eff Med Implants*, 15:39–47.
- Miller DC, Haberstroh KM, Webster TJ. 2004. Endothelial and vascular smooth muscle cell function on poly(lactic-co-glycolic acid) with nano-structured surface features. *Biomaterials*, 25:53–61.
- Miller DC, Haberstroh KM, Webster TJ. 2005. Mechanisms of increased vascular cell responses on nanostructured polymers. *J Biomed Mater Res*. In press.
- National Institutes of Health. 2005. [online]. Accessed 16 May 2005. URL: <http://www.nlm.nih.gov/medlineplus>.
- Pitt WG, Morris RN, Mason ML, et al. 2004. Attachment of hyaluronan to metallic surfaces. *Biomaterials*, 68:95–106.
- Robertson SW, Imbeni V, Wenk HR, et al. 2005. Crystallographic texture for tube and plate of the superelastic/shape-memory alloy Nitinol used for endovascular stents. *J Biomed Mater Res*, 72A:190–9.
- Schuler P, Assefa D, Ylanne J, et al. 2003. Adhesion of monocytes to medical steel as used for vascular stents is mediated by the integrin receptor Mac-1 (CD11b/CD18; alphaM beta2) and can be inhibited by semiconductor coating. *Cell Commun Adhes*, 10:17–26.
- Siegel RW. 1996. Creating nanophase materials. *Sci Am*, 275:42.
- Sung H-K, Su J, Berglund JD, et al. 2005. The use of temperature-composition combinatorial libraries to study the effects of biodegradable polymer blend surfaces on vascular cells. *Biomaterials*, 26: 4557–67.
- Webster TJ, Ejiófor JU. 2004. Increased osteoblast adhesion on nanostructured metals. *Biomaterials*, 25: 4731–9.

